



INSTITUT
Mines-Télécom

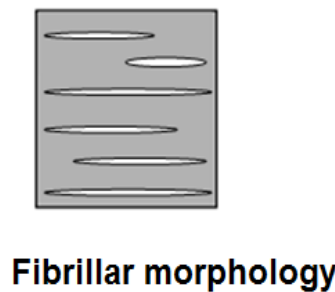
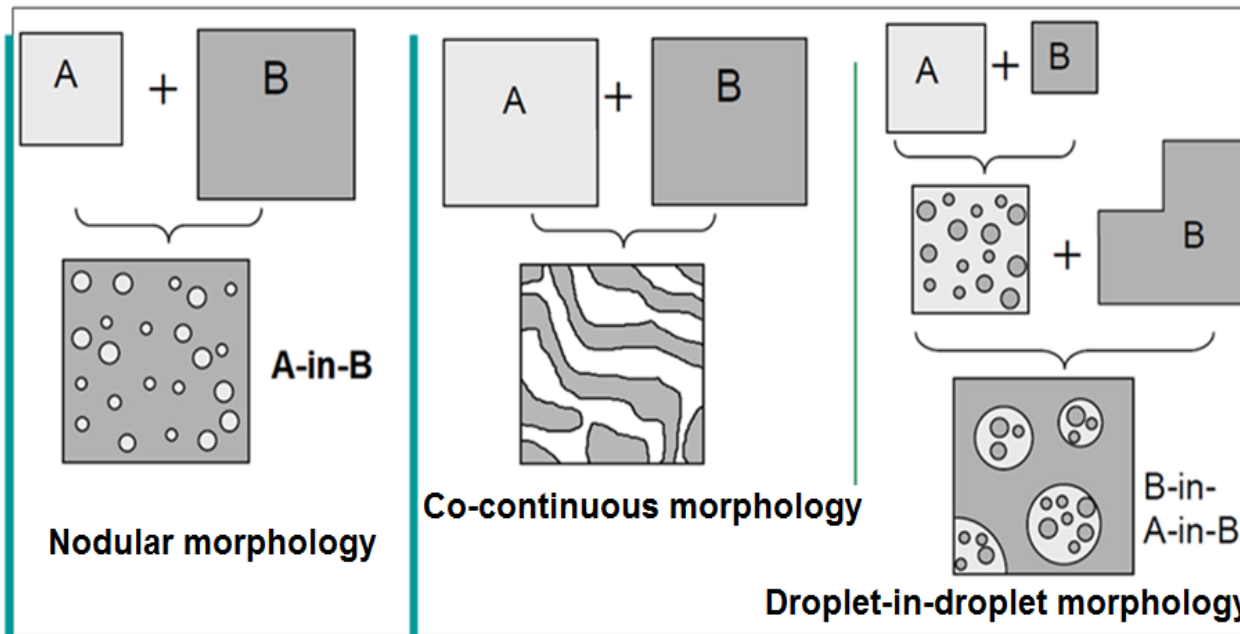
Systèmes polymères multiphasés : des polymères de commodité vers les polymères de performance, par le contrôle des propriétés interfaciales et des procédés de mise en œuvre et mise en forme

Prof. J. SOULESTIN, dpt TPCIM,
Mines Douai

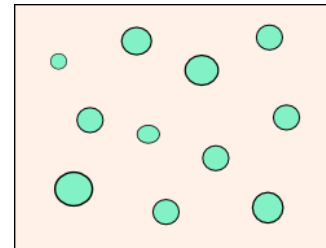


INTRODUCTION

Immiscible polymer blends: various possible morphologies

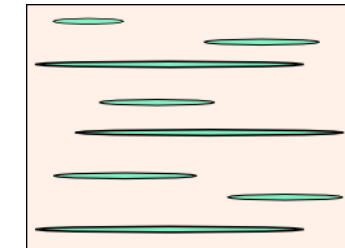


Fibrillar morphology



Fibrillation in-situ

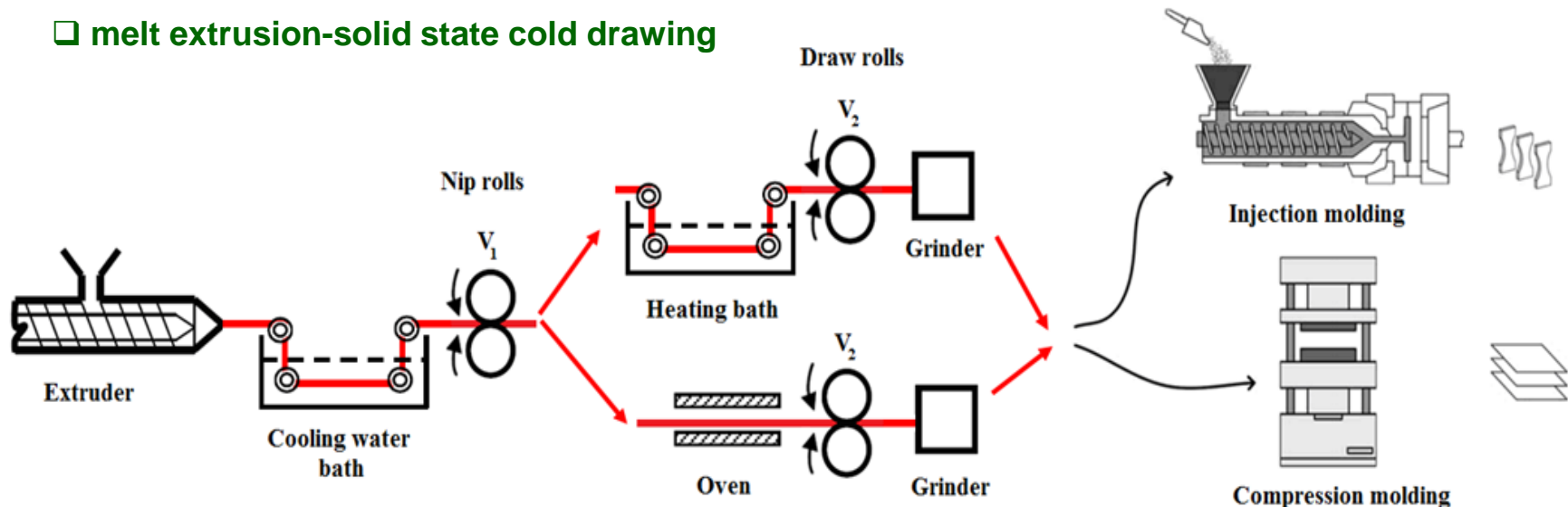
Écoulement élongationnel



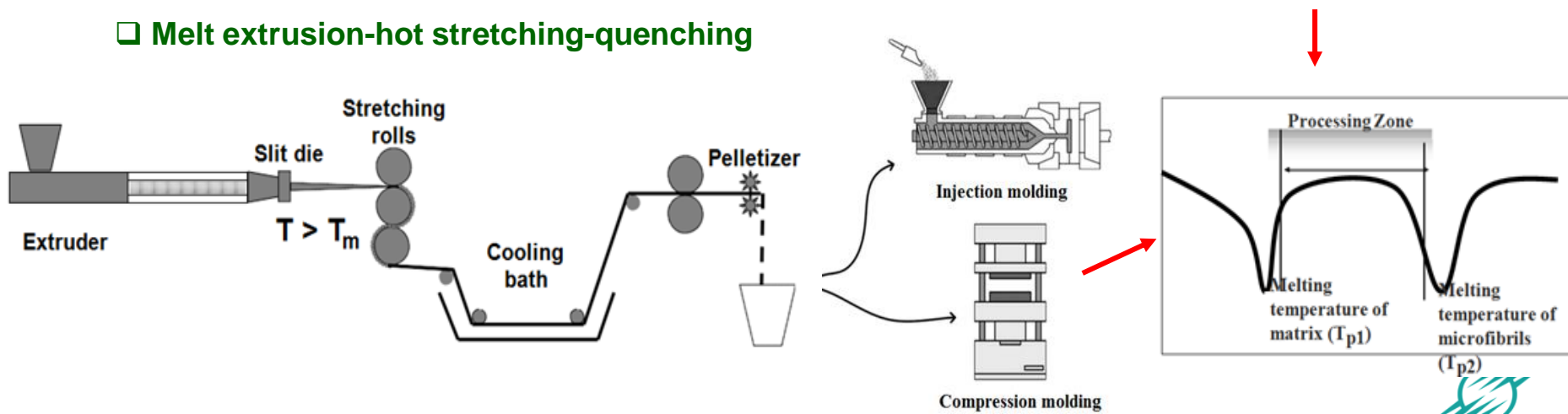
INTRODUCTION

Different industrial approaches to prepare in-situ microfibrillar TP/TP composites

□ melt extrusion-solid state cold drawing



□ Melt extrusion-hot stretching-quenching



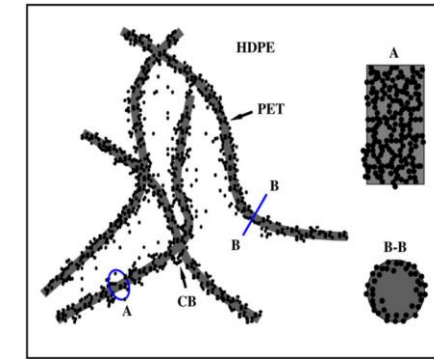
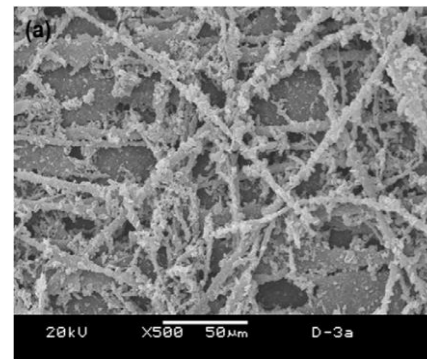
INTRODUCTION

Potential applications of MFC technology

□ MFC technology for recycling of plastics

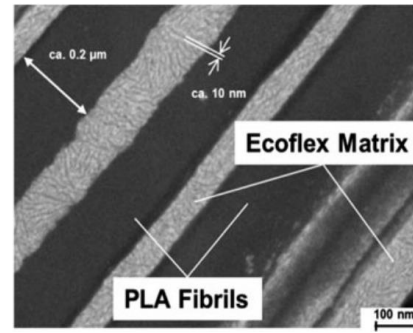
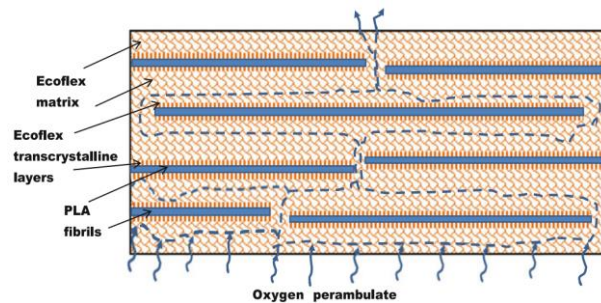
MFCs have good application potentials in the car manufacturing industry, particularly in Europe due to the initiation of ecological regulations and legislation such as the *European Union End-of-Life Vehicles regulation*.

□ Conducting composites



Polymer 2007; 48 ; 849.

□ Packaging applications

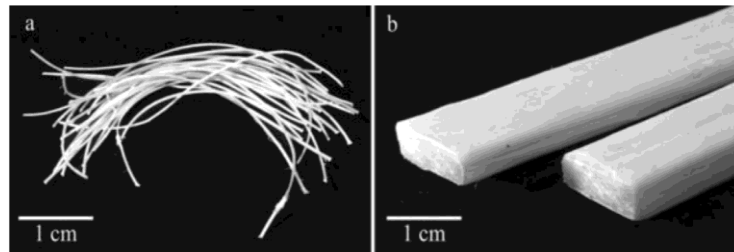


J Mater Sci. 2013, 48, 6312.

INTRODUCTION

Potential applications of MFC technology

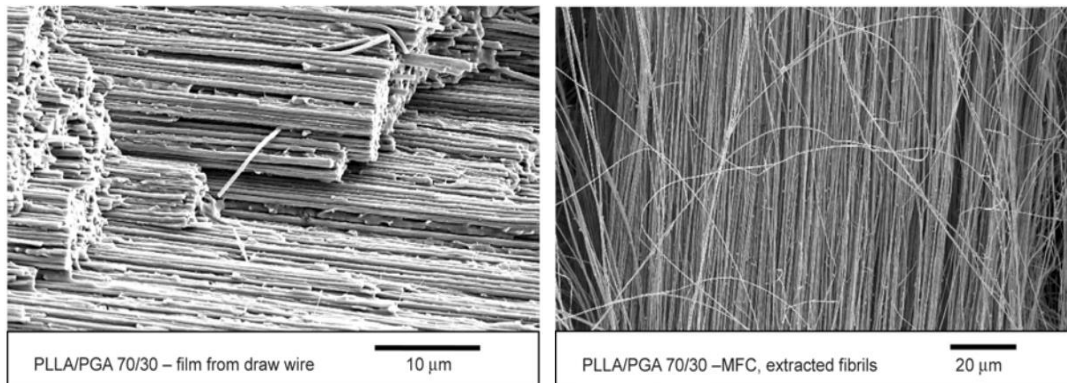
□ Pultruded products



Polym. Eng. Sci. 2010, 50, 402.

□ Biomedical application

Isolation of bio-microfibrils via selective dissolution of the matrix component offers the potential for their biomedical applications as scaffolds for regenerative medicine or in controlled drug delivery or as biodegradable coronary stents .

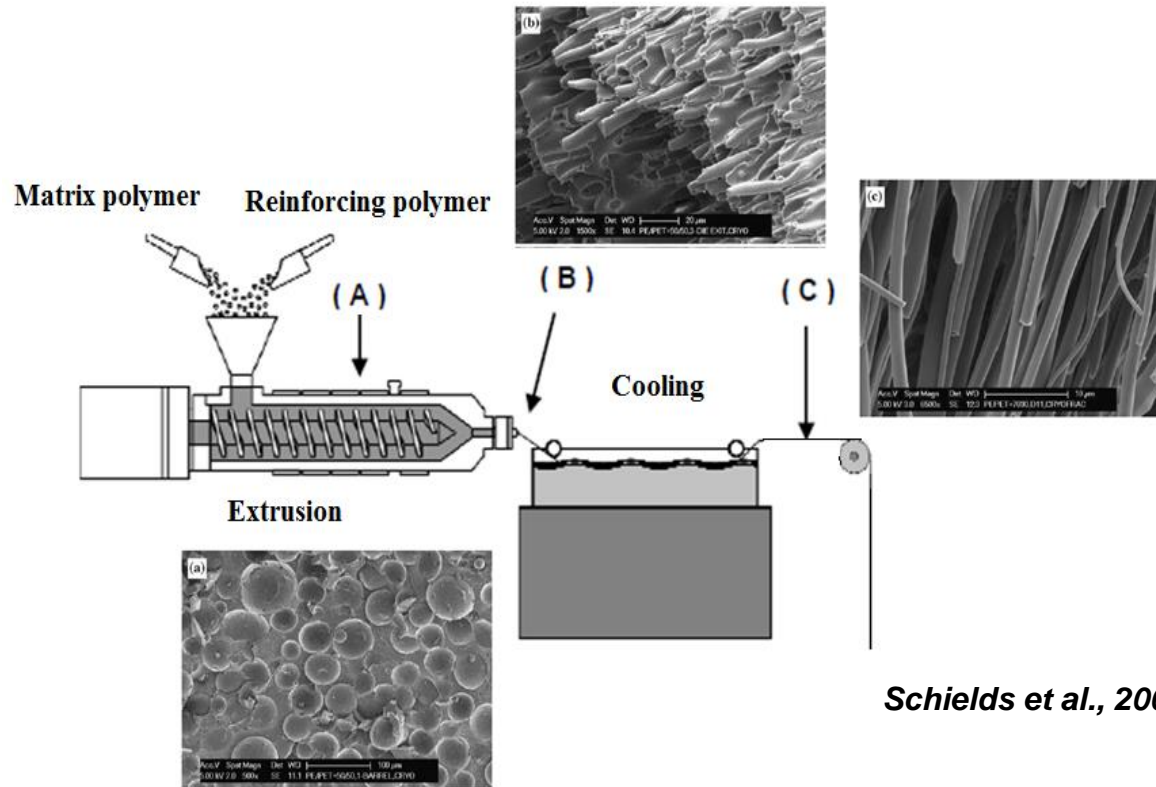


Biodegradable microfibrillar polymer-polymer composites from poly(L-lactic acid)/poly(glycolic acid)

Express Polymer Letters, 2015, 9, 300

Theory of deformation and break-up of droplets in immiscible polymer blends

Morphological evolution of in-situ microfibrillar composites during processing



Preparing in-situ fibril-reinforced materials during processing (extrusion or injection molding) requires careful selection of rheological conditions necessary to produce the fibrillation of the minor phase.

Theory of deformation and break-up of droplets in immiscible polymer blends

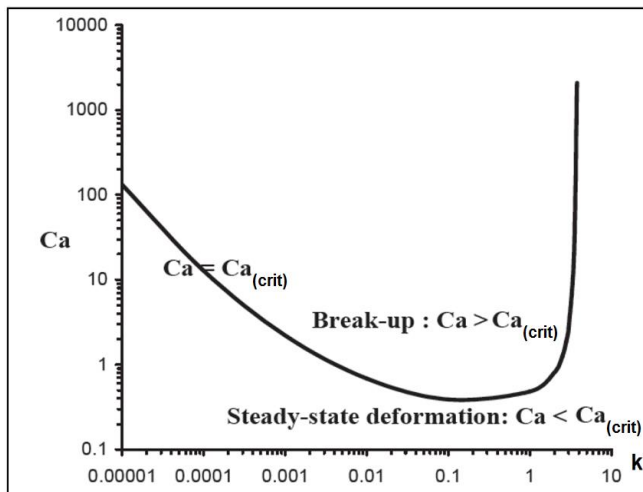
Case of Newtonian drop in Newtonian matrix

➤ Critical capillary number $Ca_{(crit)}$ in the case of **Newtonian fluids**

$$Ca = \frac{\eta_m \cdot \gamma}{\Gamma / R} \quad G.I. Taylor. Proc. R. Soc. London 1934. A146. 501.$$

At drop breakup: $\dot{\gamma} = \dot{\gamma}_{(crit)}$

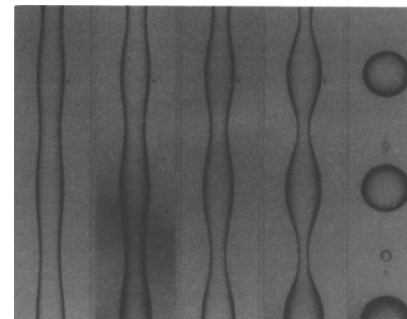
$$\rightarrow Ca = Ca_{(crit)} = \frac{\eta_m \cdot \dot{\gamma}_{(crit)}}{\Gamma / R}$$



HP. Grace. Chemical Engineering Communications. 1982, 14, 225.

Favorable conditions to obtain a fibrillar morphology

- Viscosity ratio (k) < 4 (HP. Grace. 1982)
- Elasticity ratio (k') < 1 (Mighri et al. 1998)
- Break-up (tb) >> relaxation time (λ) (Stegeman., 2002)
- Break-up time (tb) >> crystallization time ($t_{1/2}$) (Fulchiron, 2002)



Sinusoidal distortions on a polyamide 6 thread (diameter 55 μm) embedded in a PS matrix at 230 °C (Elemans et al., 1990).

The photographs were taken at: $t = 0, 15, 30, 45, 60$ s.

$$\log(Ca_{(crit)}) = -0.506 - 0.0994 \log(k) + 0.124 (\log(k))^2 - \frac{0.115}{\log(k) - 0.6107}$$

R.A. de Bruijn. PhD thesis, Eindhoven University of Technology, The Netherlands, 1989.

Case of non-Newtonian fluids

- Critical capillary number in the case of **non-Newtonian fluids**

$$Ca_{(crit)} = \frac{\eta_m \cdot \dot{\gamma}_{(crit)}}{\Gamma / R}$$

- ✓ Elastic effect of the dispersed phase

U. Sundararaj and C.W. Macosko. Macromolecules, 1996,28, 2647.

The break-up will occur when:

Shear stress $\rightarrow \eta_m \cdot \dot{\gamma} - N_{1,d} > Ca_{crit} \cdot (2 \cdot \Gamma / D)$

- ✓ Elastic effect of the dispersed phase and the matrix (continuous phase)

Y. Seo and J. Kim. Polymer, 2001,42, 5029

$$Ca^{Elastic} = \frac{N_{1,m} - N_{1,d}}{2 \Gamma / D}$$

Dispersed particles are deformed when $Ca^{Elastic} > 1$

P. Ghodgaonkar and U. Sundararaj. Polymer Engineering and Science, 1996,36, 1656.

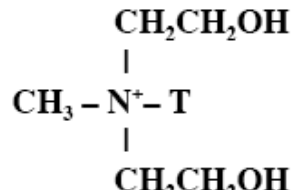
The break-up will occur when:

$$\eta_m \cdot \dot{\gamma} + N_{1,m} > \frac{2\Gamma}{D} + N_{1,d}$$

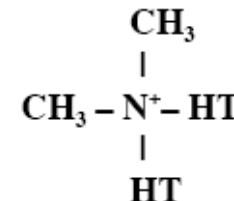
shear forces + matrix elasticity > interfacial forces + droplet elasticity

Elaboration of PP/PA/Clay blends using direct compounding

- MB route: no information on the formulation of the materials
- Influence of the type of surfactant
 - **Cloisite® 15A: better affinity with polyolefins**
 - **Cloisite® 30B: better affinity with polar polymers like PA**

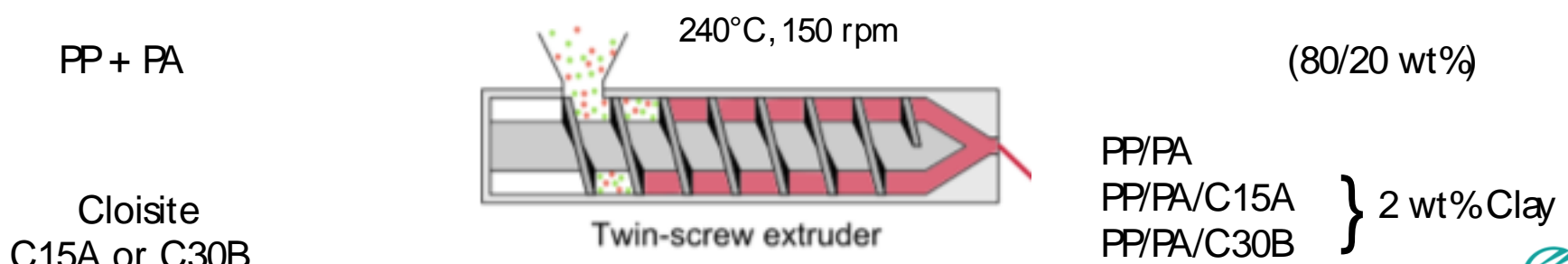


C30B surfactant



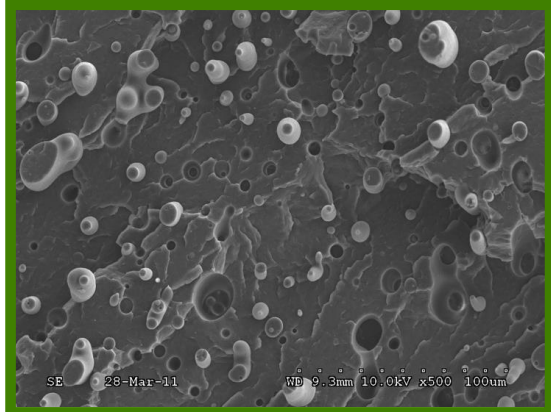
C15A surfactant

■ Processing method



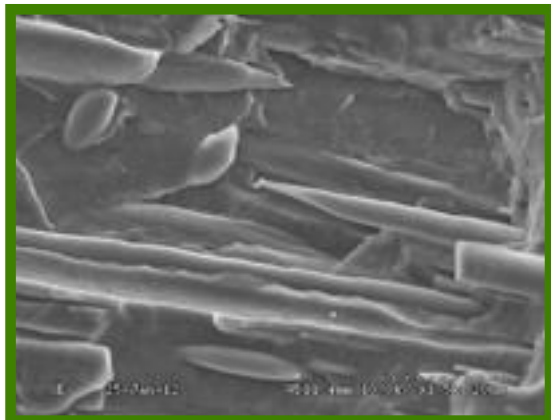
Morphology of PP/PA/Clay blends obtained using direct compounding

PP/PA blend

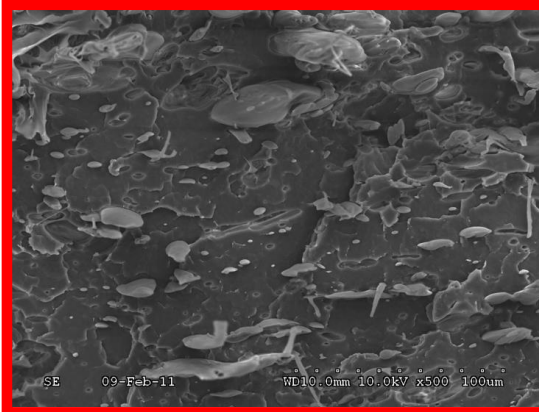


Transverse

Longitudinal

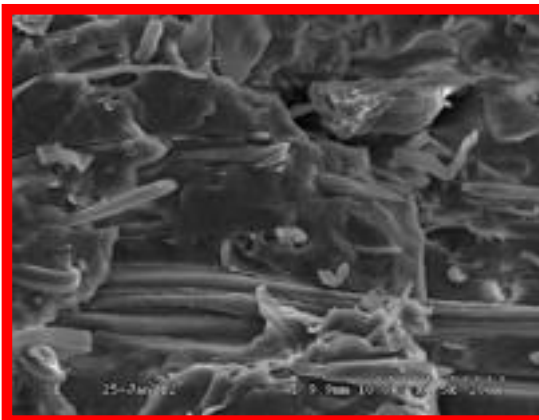


PP/PA/C30B

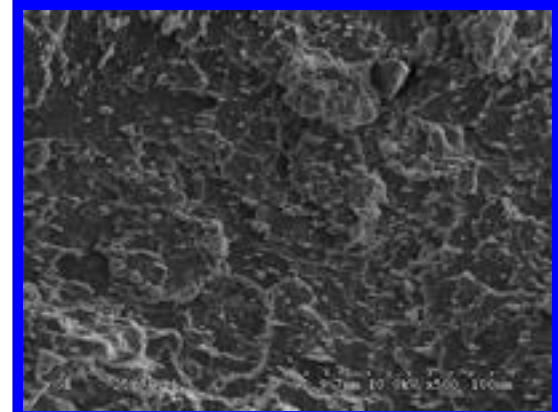


Transverse

Longitudinal

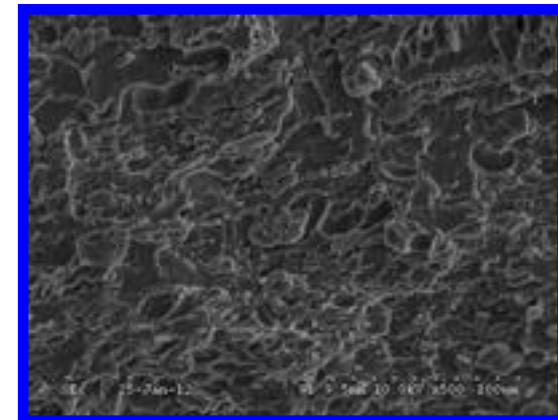


PP/PA/C15A



Transverse

Longitudinal

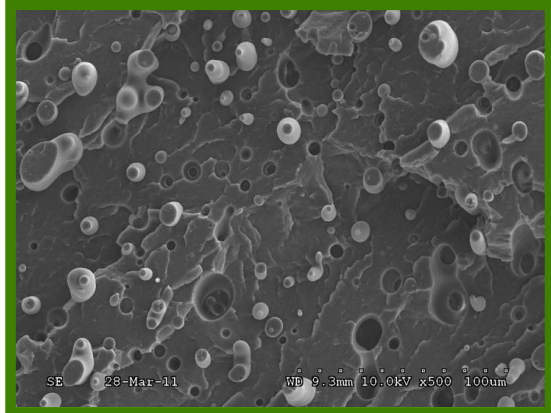


□ morph. homogeneity

destruction of fibrillar
structure with clay

Morphology of PP/PA/Clay blends obtained using direct compounding

PP/PA blend

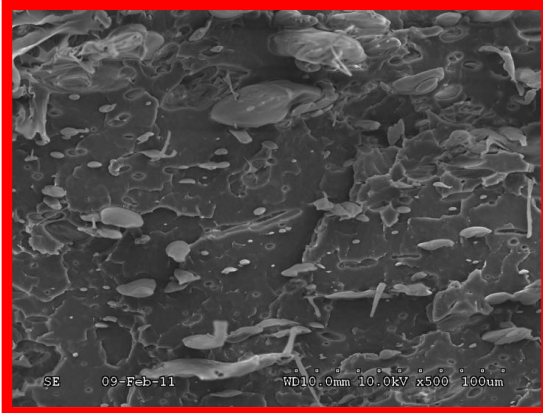


Transverse

Longitudinal

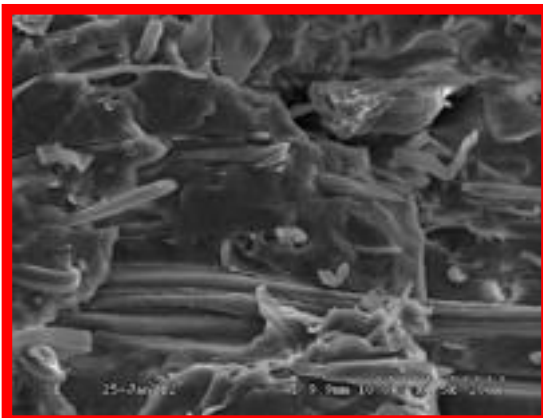


PP/PA/C30B

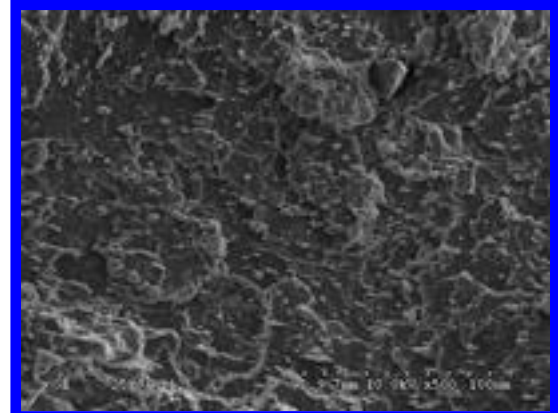


Transverse

Longitudinal

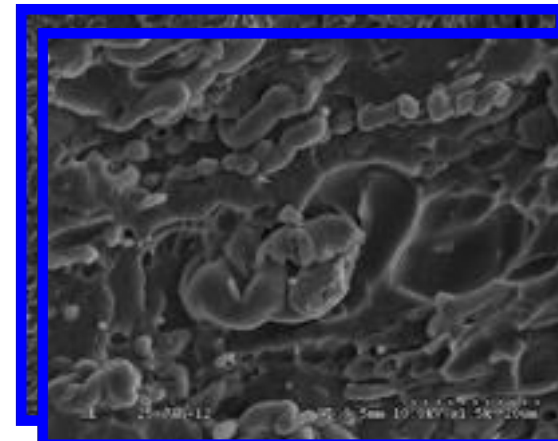


PP/PA/C15A



Transverse

Longitudinal

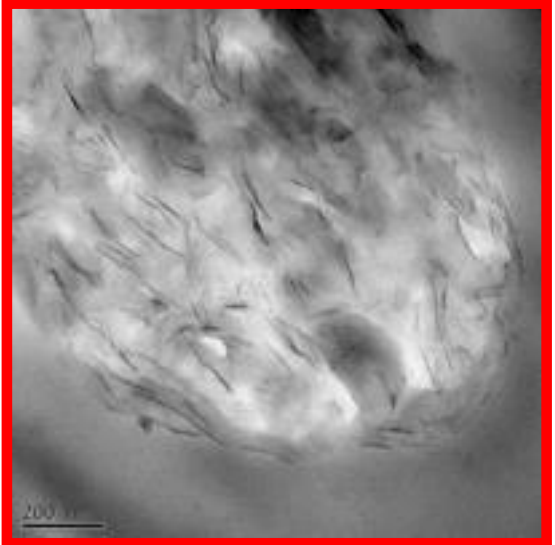
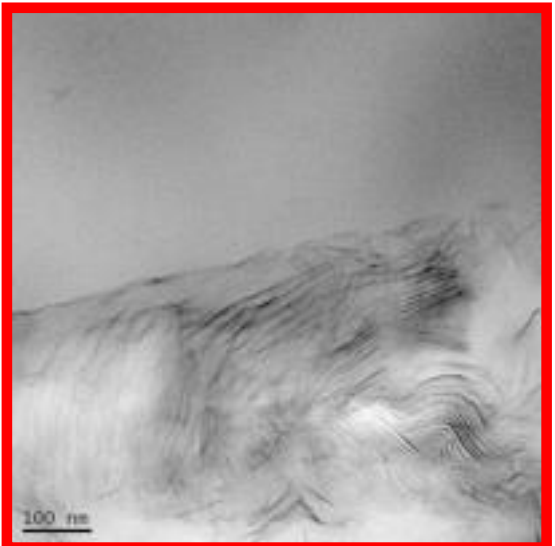


□ morph. homogeneity

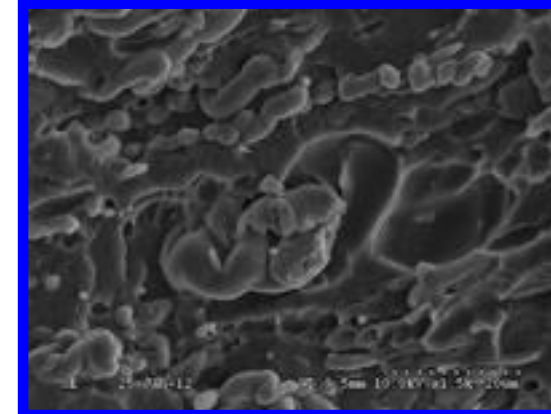
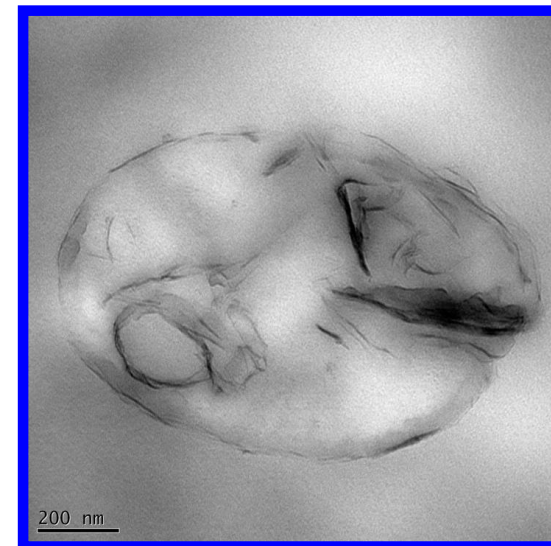
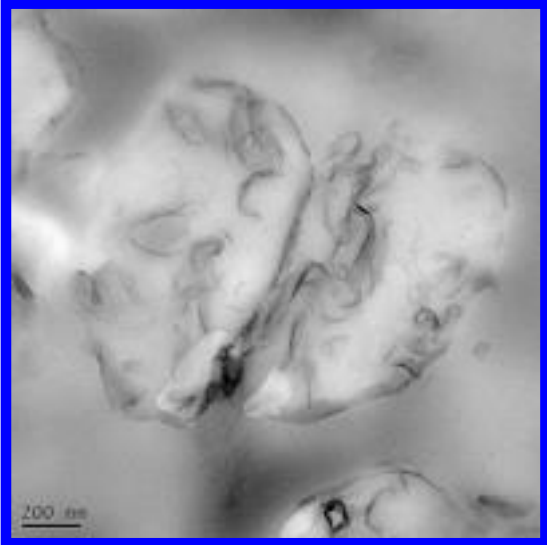
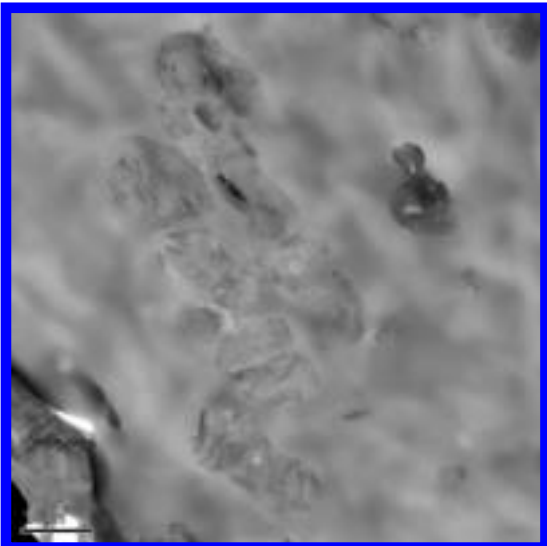
destruction of fibrillar structure with clay

Dispersion and localization of clay in PP/PA/Clay blends obtained using direct compounding

PP/PA/C30B

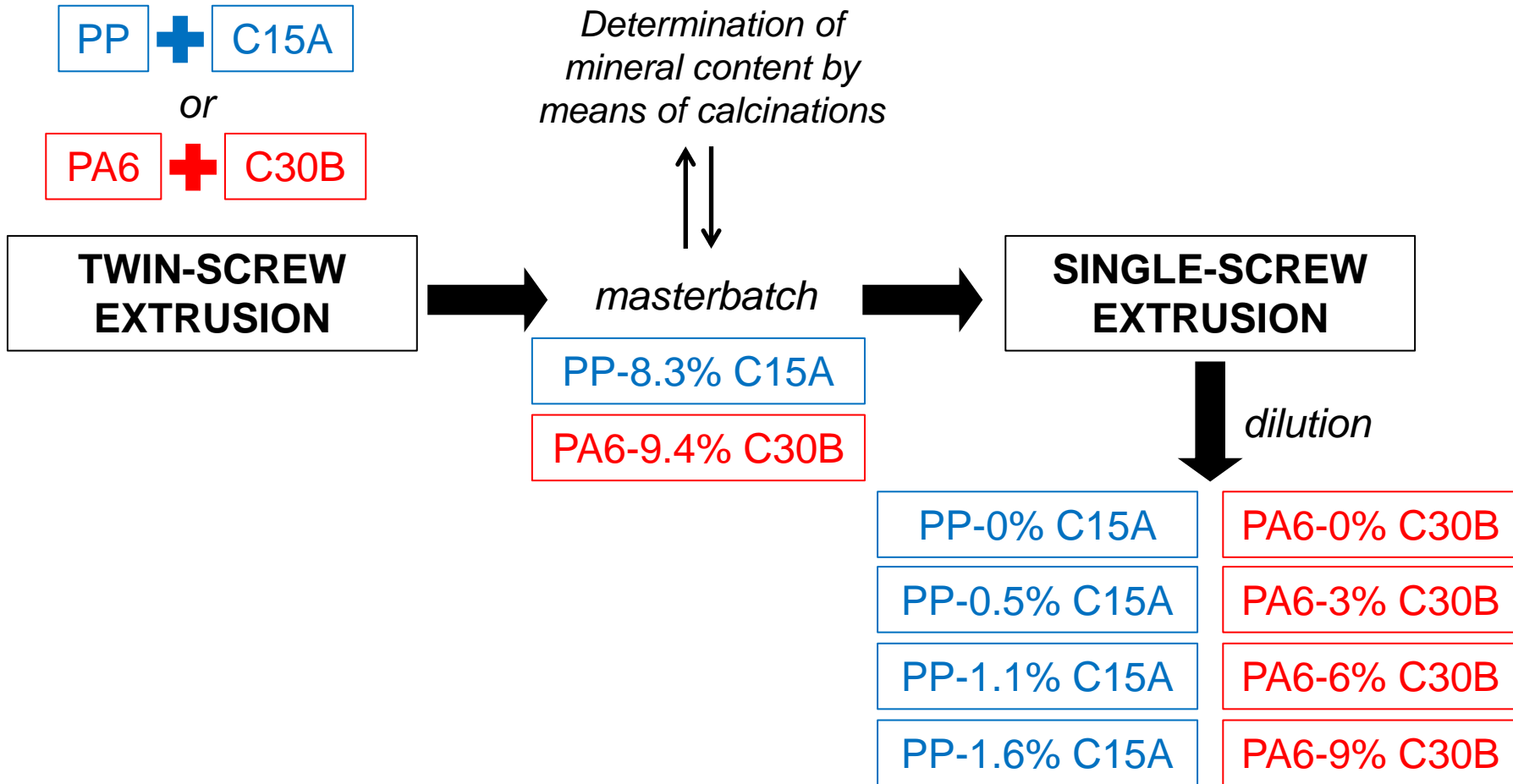


PP/PA/C15A



Localization of clay in PA6 phase for C15A/C30B

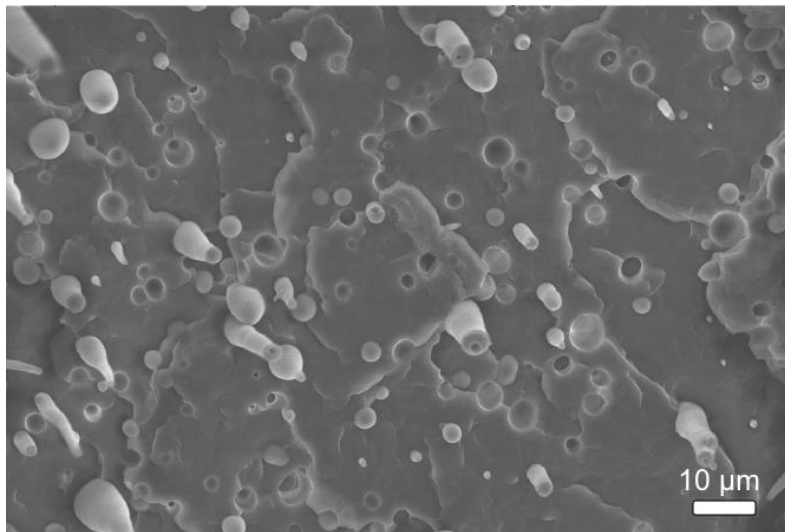
Elaboration of polymer/organoclay blends



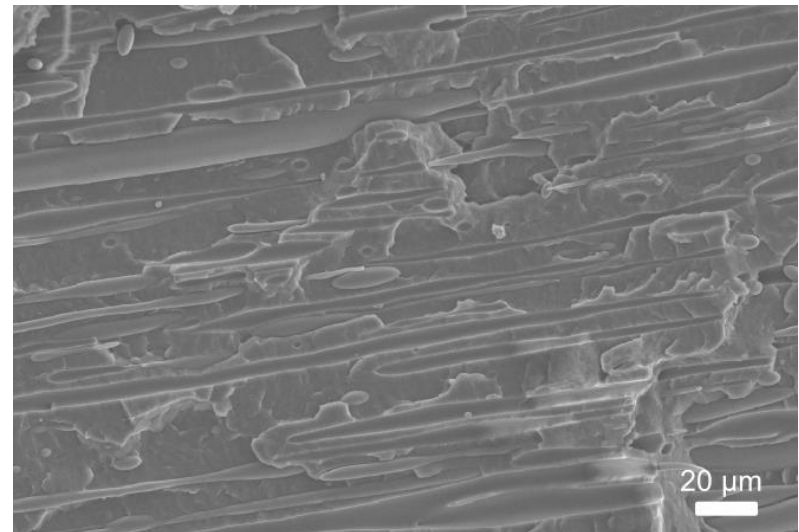
“% C15A” and “% C30B” stand for % montmorillonite arising from C15A or C30B (i.e. mineral fraction).

Morphology: PP/PA6

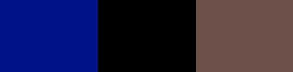
Transversal



Longitudinal

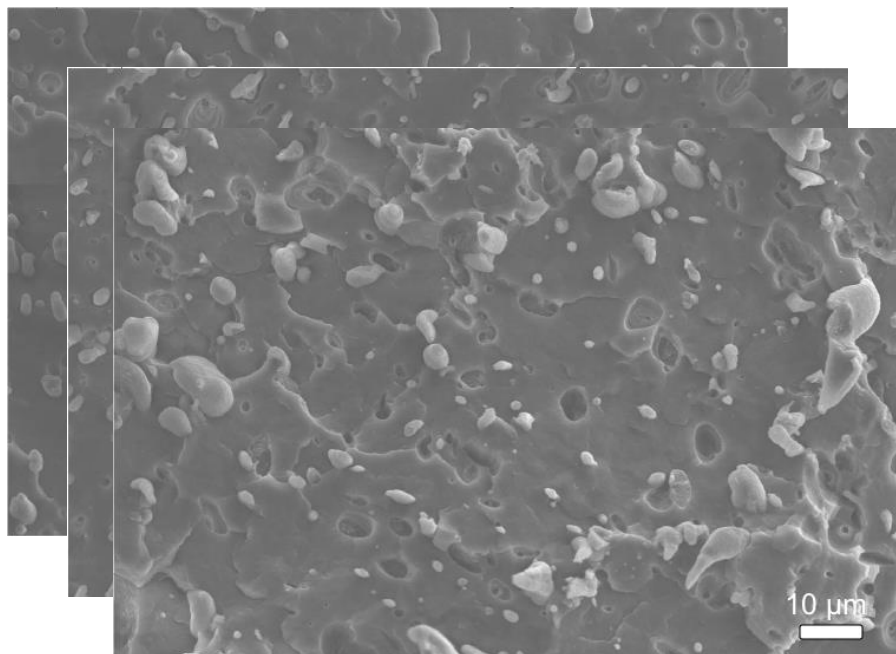


→ Fibrillar morphology with high interfacial tension



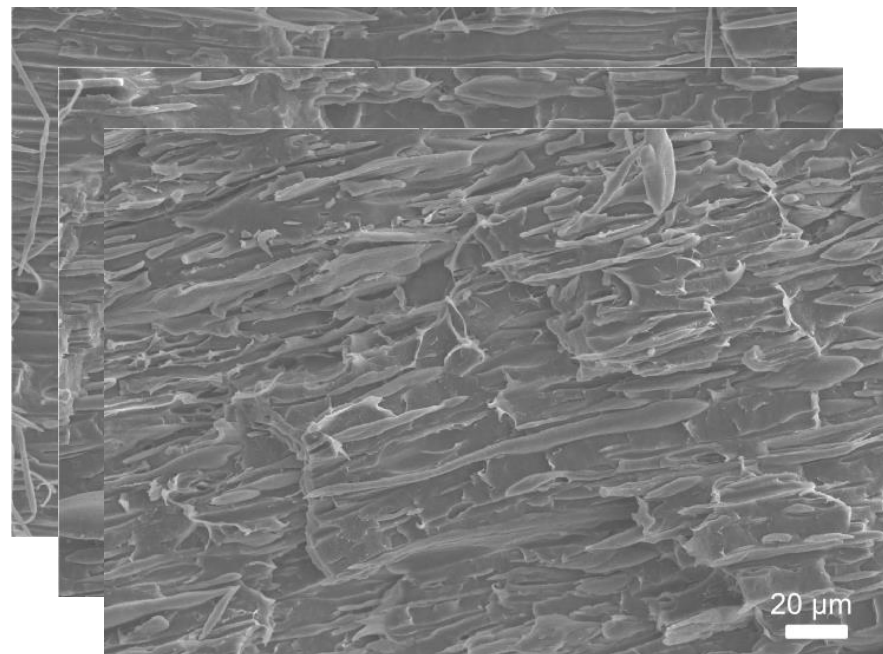
Morphology: PP/PA6/C15A

Transversal



**0.45% clay
0.9% clay
1.35% clay**

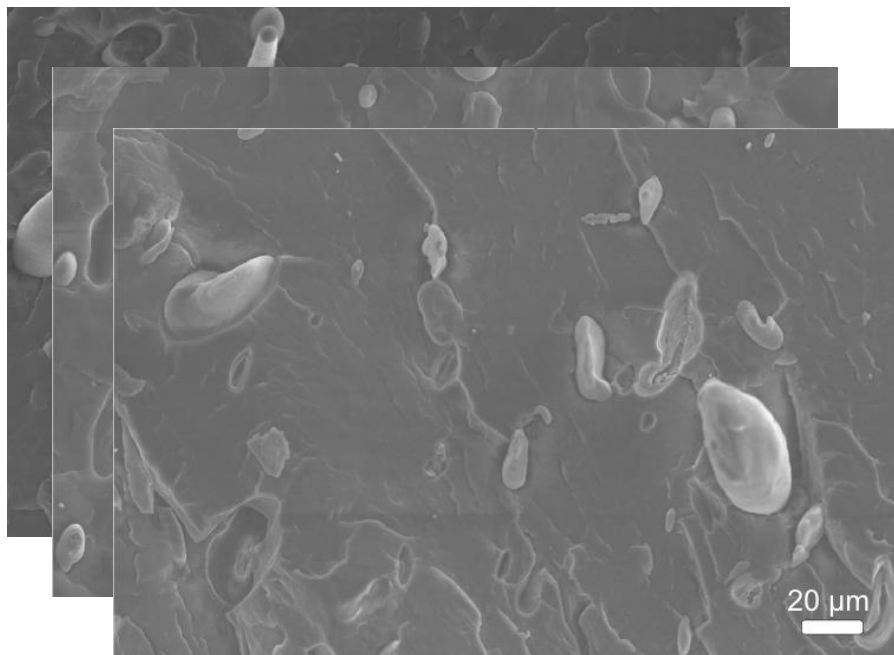
Longitudinal



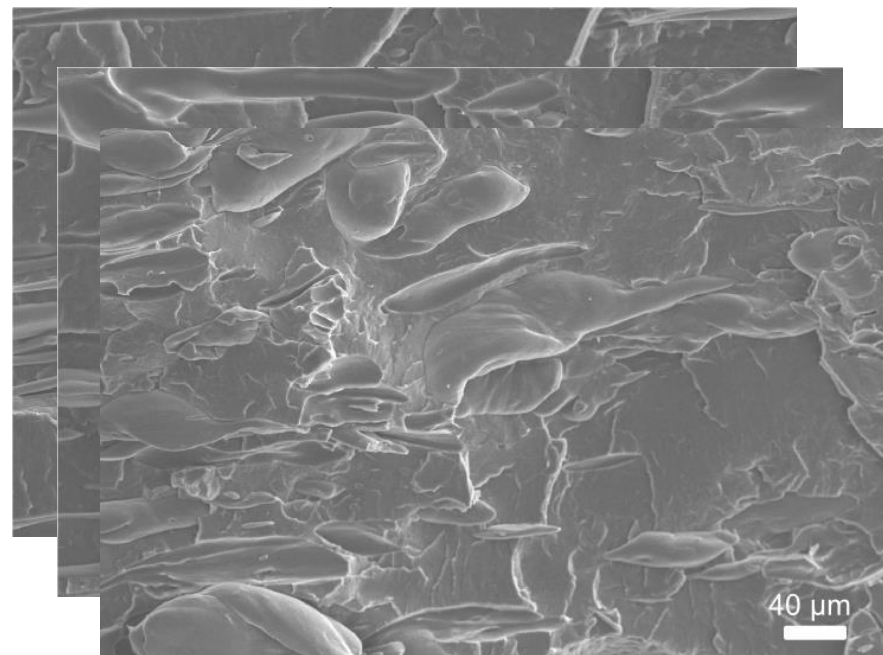


Morphology: PP/PA6/C30B

Transversal

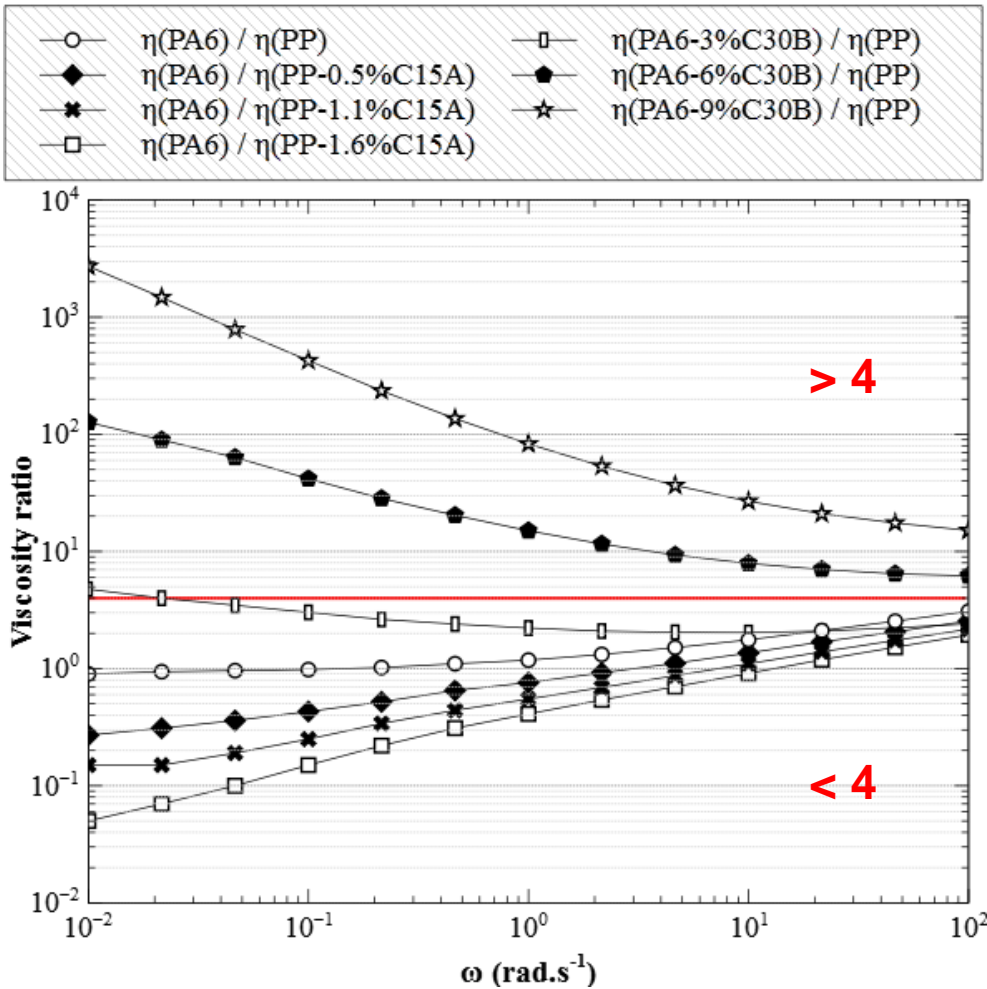


Longitudinal



0.45% clay
0.9% clay
1.35% clay

Viscosity ratio



| At 100 rad.s ⁻¹ : | Viscosity ratio |
|--|-----------------|
| $\eta(\text{PA6}) / \eta(\text{PP})$ | 3.1 |
| $\eta(\text{PA6}) / \eta(\text{PP}-0.5\% \text{C15A})$ | 2.6 |
| $\eta(\text{PA6}) / \eta(\text{PP}-1.1\% \text{C15A})$ | 2.2 |
| $\eta(\text{PA6}) / \eta(\text{PP}-1.6\% \text{C15A})$ | 1.9 |
| $\eta(\text{PA6}-3\% \text{C30B}) / \eta(\text{PP})$ | 2.4 |
| $\eta(\text{PA6}-6\% \text{C30B}) / \eta(\text{PP})$ | 6.2 |
| $\eta(\text{PA6}-9\% \text{C30B}) / \eta(\text{PP})$ | 15.1 |

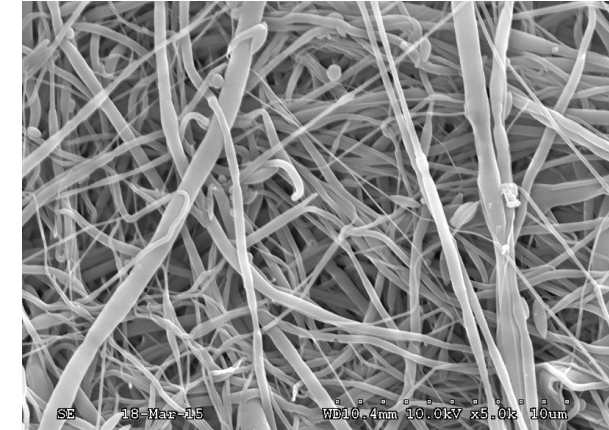
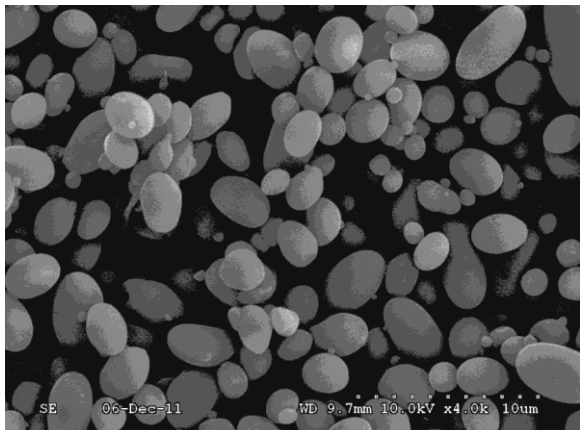
→ Having the clay dispersed in the minor phase affects strongly the viscosity ratio.

Elaboration of PLA/PA11 blends with fibrillar morphologies

85 % PLA
15 % PA11



→ Chemical etching for SEM morphological observations



PLA/PA11 nodular morphology

→ No in-situ fibrillation

Decrease of η_{PA11}

→ Partial fibrillation

Increase of η_{PLA}

→ Fibrillation

Fibrillation = very high ductility

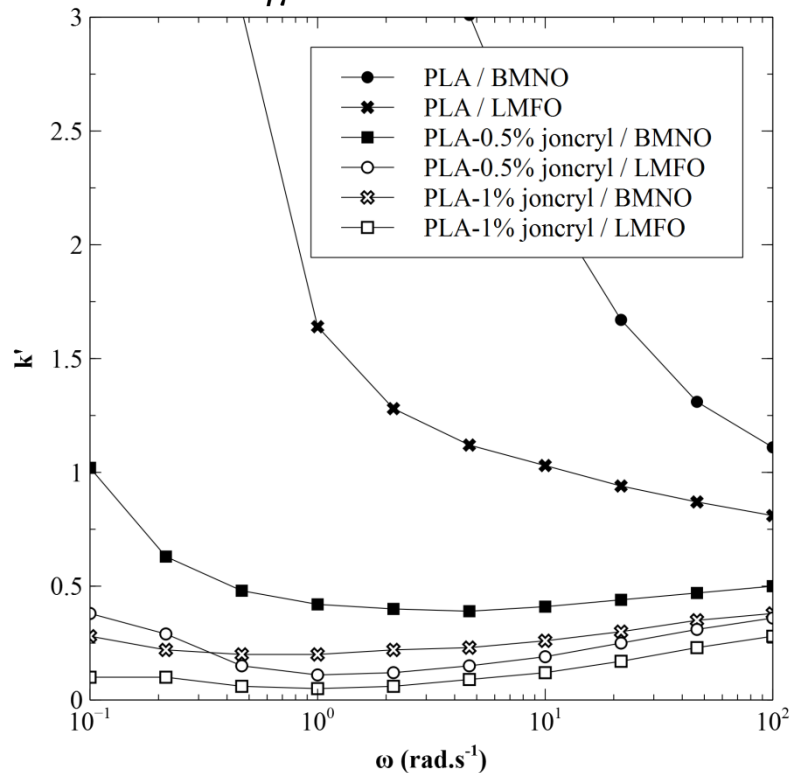
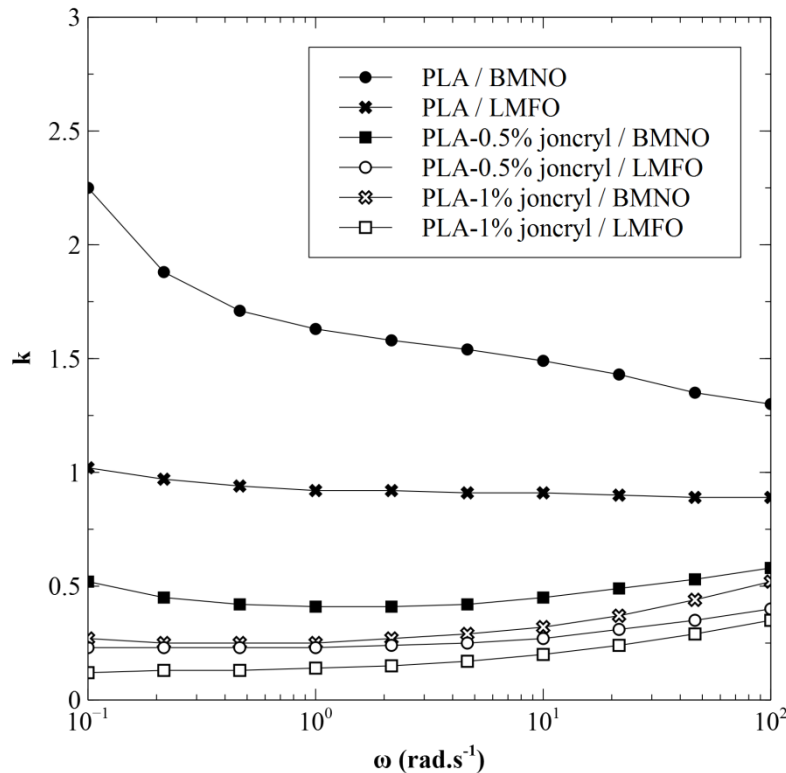
Viscosity and elasticity of PLA/PA11 blends at 200°C

$k = \frac{| \text{phase minoritaire} |}{| \text{matrice} |}$

$k' = \frac{| \text{phase minoritaire} |}{| \text{matrice} |}$

$$\text{avec } \lambda = \frac{N_1}{2\eta\dot{\gamma}^2}$$

Mighri, Journal of Rheology (1998)

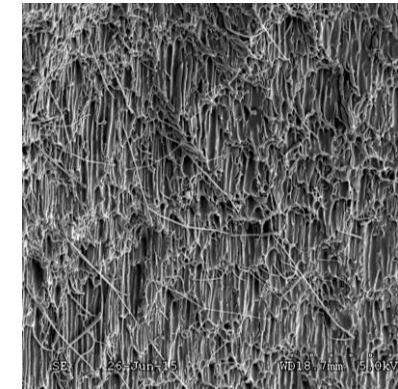
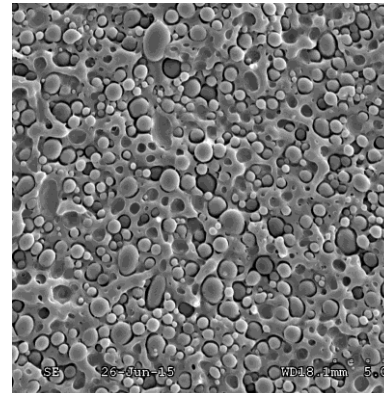


Different blends with k and k' : >1; =1; ou <1.



Prof. Patricia Krawczak

Dr. Mohamed Yousfi
Dr. Dimitri Chomat
Dr. David Lemeny
Prof. M-F. Lacrampe
Dr. Eric Lafranche
Dr. Kalappa Prashantha
Dr. Cedric Samuel
Laurent Charlet
Dr. Catherine Douchain
Carlo Angotzi
Thierry Chevalier
Murielle Delsert
Bernard Pauchet
Jean-Michel Pollet



TPCIM
Technologie des
Polymères et
Composites &
Ingénierie Mécanique

